Int. J Multiphase Flow Vol 12, No 4, pp 587–608, 1986
Printed in Great Britain

0301-9322/86 $3.00 + .00
Pergamon Journals/Elsevier

TWO-PHASE FLOW IN A *T*-JUNCTION WITH A HORIZONTAL INLET

PART II: PRESSURE DIFFERENCES

J. REIMANN and W. SEEGER
Kernforschungszentrum Karlsruhe, Institut für Reaktorbauelemente, Postfach 3640, 7500 Karlsruhe 1, Federal Republic of Germany

(*Received* 31 *May* 1985; *in revised form* 10 *October* 1985)

Abstract—The pressure differences between pipe inlet and run, Δp_{1-2}, and inlet branch, Δp_{1-3}, were measured for air–water and steam–water flow in a *T*-junction with equal diameters and a horizontal, vertical upward or downward branch. The experimental results are compared with those previously published and a model presented herein. The agreement is good for the horizontal and vertical downward branch; however, no model predicts satisfactorily the pressure drop in the upward branch flow

1. INTRODUCTION

When a flow is divided in a *T*-junction the deceleration of the fluid causes a reversible pressure rise in the run and in the branch due to the Bernoulli effect. However, in our experiment the reversible pressure rise in the branch was smaller than the irreversible pressure drop; therefore, the resultant pressure difference Δp_{1-3} between inlet and branch has a positive sign and is equivalent to a pressure drop, whereas in the run the irreversible pressure drop is considerably smaller and therefore Δp_{1-2} typically has a negative sign, characterizing a pressure rise (the subscripts 1, 2, or 3 refer to the inlet, run, or branch conditions).

If a two-phase flow is divided, in general, phase separation occurs. The degree of phase separation must be known to model the pressure differences. In Part I of this article results on phase separation were presented, whereas in this part the corresponding pressure difference results are discussed.

Only a few experiments were performed previously with elaborate differential pressure measurements along the axis of the inlet, branch, and run of the pipe which enable us to properly separate the *T*-junction pressure differences from the frictional and gravitational pressure differences.

Fitzsimmons (1964) performed steam–water experiments with a horizontal *T*-junction (all pipes in a horizontal plane) with inlet mass fluxes $1000 < G < 5000\ \mathrm{kg/m^2s}$. However, only the mass flux ratio G_3/G_1 equal to unity was investigated. Chisholm (1967) used these data for deriving his pressure drop model, presented in section 2.

Saba & Lahey (1982, 1984) reported on air–water experiments with a horizontal *T*-junction. The inlet mass fluxes were $G_1 = 1350$, 2035, and $2700\ \mathrm{kg/m^2s}$ and the mass flux ratios were $G_3/G_1 = 0.3$, 0.5, and 0.7. The models derived by these authors to predict the pressure differences will also be discussed in section 2.

Reimann & Seeger (1983) presented a model for the branch pressure drop Δp_{1-3} and compared the predictions with air–water experiments using a horizontal *T*-junction. In this article this model is extended to predict also the pressure difference Δp_{1-2}. This model and other models are compared with measurements in air–water and steam–water flow.

2. SINGLE-PHASE FLOW

The pressure differences Δp_{1-2} and Δp_{1-3} are commonly written as a sum consisting of the reversible pressure increase and the irreversible pressure drop (see e.g. VDI 1984; Collier 1976):

$$\Delta p_{1-i} = (\Delta p_{1-i})_{\mathrm{rev}} + (\Delta p_{1-i})_{\mathrm{irr}}, \qquad [1]$$

with $i = 2$ for the run and $i = 3$ for the branch, where

$$(\Delta p_{1-i})_{\text{rev}} = \frac{1}{2}\left(\frac{G_i^2}{\rho_i} - \frac{G_1^2}{\rho_1}\right) \quad [2]$$

and

$$(\Delta p_{1-i})_{\text{irr}} = K_{1i}\left(\frac{G_1^2}{2\rho_1}\right), \quad [3]$$

where ρ is the fluid density, K_{12} and K_{13} are loss coefficients depending on the mass flux ratio G_3/G_1 which corresponds to a volume flow rate ratio $\dot{V}_3/\dot{V}_1$.

Another method to model the pressure difference Δp_{1-3} is to split it into a reversible pressure difference Δp_{1-c_3} between inlet 1 and the throat of the vena contracta c_3 and a pressure difference Δp_{c_3-3} between c_3 and a position 3 downstream in the branch, modeled according to a sudden expansion (compare figure 1). Therefore we get

$$\Delta p_{1-c_3} = \frac{1}{2}\left(\frac{G_{c_3}^2}{\rho_{c_3}} - \frac{G_1^2}{\rho_1}\right) \quad [4]$$

and

$$\Delta p_{c_3-3} = \frac{G_3^2}{\rho_3} - \frac{G_3\, G_{c_3}}{\rho_3}. \quad [5]$$

By eliminating G_{c_3} using the relationship for the conservation of mass and by introducing a contraction coefficient $C_3 = A_c/A$, where A is the total cross section, we obtain for $\rho_{c3} = \rho_3$,

$$\Delta p_{1-3} = \frac{1}{2}\left(\frac{G_3^2}{\rho_3} - \frac{G_1^2}{\rho_1}\right) + \left(\frac{1}{C_3} - 1\right)^2 \frac{G_3^2}{2\rho_3}. \quad [6]$$

Comparing [1]–[3] with [6] results in the following relationship between C_3 and K_{13}:

$$C_3 = \left(1 + \sqrt{\frac{\rho_1}{\rho_3}}\,\frac{\dot{V}_1}{\dot{V}_3}\sqrt{K_{13}}\right)^{-1}. \quad [7]$$

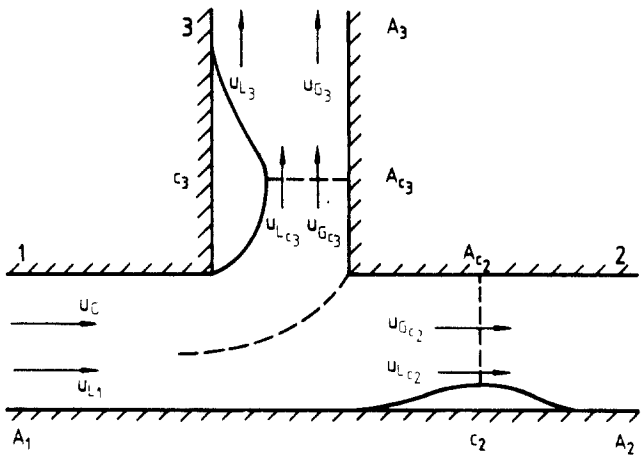

Figure 1 Two-phase through a T-junction

For incompressible flow ρ_1 is equal to ρ_3. A comparison of C_3, determined from two-dimensional potential theory (compare, e.g. Sallet & Popp 1983) and the right side of [7], using experimental results for K_{13} shows good agreement. Therefore, this procedure for modeling the pressure drop seems to be physically reasonable and will be applied later.

If in an analogous way the pressure difference Δp_{1-2} is modeled, relationships identical to [6] and [7] are obtained except that the index 3 is replaced by the index 2. The existence of a vena contracta in the run (compare figure 1) is impressively shown in the textbook of Hackeschmidt (1970).

3. PREVIOUS MODELS FOR TWO-PHASE FLOW IN T-JUNCTIONS

3.1 Relationships for Δp_{1-3}

The pressure drop Δp_{1-3} is expressed according to [1]. The reversible pressure increase in its general form is written as (Saba & Lahey 1982)

$$(\Delta p_{1-3})_{\text{rev}} = \frac{\rho_{h_3}}{2}\left(\frac{G_3^2}{\rho_{e_3}^2} - \frac{G_1^2}{\rho_{e_1}^2}\right), \qquad [8]$$

where the homogeneous (ρ_{h_i}) and the energy (ρ_{e_i}) densities are given by

$$\rho_{h_i} = \left[\frac{x_i}{\rho_G} + \frac{1 - x_i}{\rho_L}\right]^{-1} \qquad [9]$$

and

$$\rho_{e_i} = \left[\frac{x_i^3}{\alpha_i^2\,\rho_g^2} + \frac{(1 - x_i)^3}{(1 - \alpha_i)^2}\frac{1}{\rho_L^2}\right]^{-2}, \qquad [10]$$

where x is the quality, α the void fraction, and ρ_L and ρ_G the liquid and gas density.

For homogeneous flow ($\rho_e = \rho_h$), [8] reduces to

$$(\Delta p_{1-3})_{\text{rev}} = \frac{\rho_{h_3}}{2}\left(\left(\frac{G_3}{\rho_{h_3}}\right)^2 - \left(\frac{G_1}{\rho_{h_1}}\right)^2\right). \qquad [11]$$

The irreversible pressure drop for homogeneous flow is written as

$$(\Delta p_{1-3})_{\text{irr}} = K_{13}\frac{G_1^2}{2\rho_{h_1}}, \qquad [12]$$

where K_{13} is taken from single-phase flow experiments. The homogeneous model, termed in the following HM, is the sum of [11] and [12].

Chisholm (1967) proposed a different relationship for $(\Delta p_{1-3})_{\text{irr}}$ which takes into account to a certain extent a velocity ratio $S > 1$:

$$(\Delta p_{1-3})_{\text{irr}} = K_{13}\frac{G_1^2}{2\rho_L}(1 - x_1)^2\left(1 + \frac{C_{1-3}^*}{X_{tt}} + \frac{1}{X_{tt}^2}\right), \qquad [13]$$

with

$$\frac{1}{X_{tt}} = \left(\frac{x_1}{1 - x_1}\right)\left(\frac{\rho_L}{\rho_G}\right)^{0.5} \qquad [14]$$

and

$$C^*_{1-3} = \left(1 + \left(C^*_3 - 1\right)\left(\frac{\rho_L - \rho_G}{\rho_L}\right)^{0.5}\right)\left(\left(\frac{\rho_L}{\rho_G}\right)^{0.5} + \left(\frac{\rho_G}{\rho_L}\right)^{0.5}\right). \quad [15]$$

For nonhomogeneous flow $C^*_3 = 1.75$ is proposed; for homogeneous flow ($C^*_3 = 1$) [13] reduces to [12].

In the following the sum of [8] and [13] will be termed the Chisholm model (CM).

Saba & Lahey (1982) obtained the best agreement of their experimental data and predictious with the homogeneous model.

Katsaounis *et al.* (1983) developed another model for the pressure drop Δp_{1-3} which also compared with the present data. This model yields satisfactory results for the mass flux ratio $G_3/G_1 = 1$ For other mass flux ratios, this model was inadequate since it predicted even larger values than the Chisholm and homogeneous models, and therefore will not be discussed.

3.2 Relationship for Δp_{1-2}

Saba & Lahey (1982) proposed a relationship which differs significantly from [1]. It is given in the general form as

$$\Delta p_{1-2} = K^*_{12}\,\frac{1}{2}\left[\left(\frac{G_2^2}{\rho_{m2}}\right) - \left(\frac{G_1^2}{\rho_{m1}}\right)\right], \quad [16]$$

where K^*_{12} is a pressure recovery coefficient determined from single-phase data and ρ_m is the momentum density given by

$$\rho_{m_i} = \left(\frac{x_i^2}{\alpha_i \rho_G} + \frac{(1 - x_i)^2}{1 - \alpha_i}\,\frac{1}{\rho_L}\right)^{-1}. \quad [17]$$

For correlating their data, Saba & Lahey used this relationship. However, they assumed a homogeneous flow:

$$\Delta p_{1-2} = \frac{1}{2} K^*_{12}\left(\frac{G_2^2}{\rho_{h2}} - \frac{G_1^2}{\rho_{h1}}\right). \quad [18]$$

4 AN IMPROVED MODEL FOR TWO-PHASE FLOW IN A *T*-JUNCTION

4.1 General formulation

Again, the pressure drop Δp_{1-3} is split into a reversible pressure difference $(\Delta p_{1-c_3})_{rev}$ and a pressure difference Δp_{c_3-3} according to a sudden expansion (compare figure 1). The conservation of energy for a nondissipative two-phase mixture with different phase velocities u_G and u_L gives

$$(p_1 - p_{c_3})\,V_3 = \frac{1}{2}\,\dot{m}_{G_3}\,(u^2_{G_{c_3}} - u^2_{G_1}) + \frac{1}{2}\,\dot{m}_{L_3}\,(u^2_{L_{c_3}} - u^2_{L_1}), \quad [19]$$

where $\dot{m}$ is the mass flow rate. Using fundamental relations such as

$$u_{G_i} = \frac{x_i\,G_i}{\alpha_i\,\rho_G}, \quad [20]$$

$$u_{L_i} = \frac{1 - x_i}{1 - \alpha_i}\,\frac{G_i}{\rho_L}, \quad [21]$$

$$\alpha_i = \frac{x_i}{x_i + (S_i/R)(1 - x_i)}, \qquad [22]$$

where S_i is the velocity ratio $S_i = u_{G_i}/u_{L_i}$, R the density ratio $R = \rho_L/\rho_G$, and assuming that $x_{c_3} = x_3$, [19] becomes

$$\Delta p_{1-c_3} = \frac{\rho_{h_3}}{2\rho_L^2}\left\{\frac{G_3^2}{C_3^2}(x_3 R + S_{c_3}(1 - x_3))^2\left(x_3 + \frac{1 - x_3}{S_{c_3}^2}\right) - G_1^2(x_1 R + S_1(1 - x_1))^2\left(x_3 + \frac{1 - x_3}{S_1^2}\right)\right\}. \qquad [23]$$

The pressure difference for a sudden expansion is given by (Collier 1976)

$$(p_{c_3} - p_3) A_3 = \dot{m}_{G_3}(u_{G_3} - u_{G_{c_3}}) + \dot{m}_{L_3}(u_{L_3} - u_{L_{c_3}}). \qquad [24]$$

Introducing [20]–[22] into [24] gives

$$\Delta p_{c_3-3} = \frac{G_3^2}{\rho_L}\left\{(x_3 R + S_3(1 - x_3))\left(x_3 + \frac{1 - x_3}{S_3}\right) - \frac{1}{C_3}(x_3 R + S_c(1 - x_3))\left(x_3 + \frac{1 - x_3}{S_c}\right)\right\}. \qquad [25]$$

As in [7], the contraction coefficient C_3 is defined as

$$C_3 = \left(1 + \sqrt{\frac{\rho_{h_3}}{\rho_{h_1}}}\frac{\dot{V}_1}{\dot{V}_3}\sqrt{K_{13}}\right)^{-1}, \qquad [26]$$

where K_{13} is taken from single-phase flow experiments as a function of the volume flow rate ratio $\dot{V}_3/\dot{V}_1$.

The corresponding expressions for the pressure difference Δp_{1-2} are obtained by replacing index 3 by index 2. In the following, simplifying assumptions are made.

4.2 Simplified relationship for Δp_{1-2}

The relationships for Δp_{1-2} contain the velocity ratios S_1, S_{c_2}, and S_2 as parameters. It seems to be reasonable to apply a correlation for well-developed flow for S_1 and S_2. However, quantitative information is not available for the velocity ratio at the vena contracta. Visual observations indicate that the flow is relatively well mixed. Therefore, a value $S_{c_2} = 1$ was assumed. Finally, the equation of the present model (termed PM) is then given by

$$\Delta p_{1-2} = \frac{\rho_{h_2}}{2\rho_L^2}\left\{\frac{G_2^2}{C_2^2}[x_2 R + (1 - x_2)]^2 - G_1^2[x_1 R + S_1(1 - x_1)]^2\left(x_2 + \frac{1 - x_2}{S_1^2}\right)\right\} \qquad [27]$$

$$+ \frac{G_2^2}{\rho_L}\left\{[x_2 R + S_2(1 - x_2)]\left(x_2 + \frac{1 - x_2}{S_2}\right) - \frac{1}{C_2}[x_2 R + (1 - x_2)]\right\},$$

with

$$C_2 = \left(1 + \left(\frac{\rho_{h_1}}{\rho_{h_2}}\right)^{0.5}\frac{\dot{V}_1}{\dot{V}_2}\sqrt{K_{12}}\right)^{-1}. \qquad [28]$$

To determine the velocity ratio, the correlation developed by Rouhani (1969) is recommended:

$$S_i = \rho_L \frac{1}{1 - x_i} \left(\frac{C^*}{\rho_{h_1}} + \frac{W_{rel}}{G_i} - \frac{x_i}{\rho_G} \right), \quad [29]$$

with

$$W_{rel} = \frac{1.18}{\sqrt{\rho_L}} (g\sigma (\rho_L - \rho_G))^{1/4} \quad [30]$$

$$C^* = 1 + 0.12(1 - x_i), \quad [31]$$

where σ is the surface tension and g the acceleration due to gravity.

4.3 Simplified relationship for Δp_{1-3}

Here parameters are S_1, S_{c_3}, and S_3. Again it appears reasonable to use a relationship for S_1 derived for well-developed flow. In the branch, however, the phase and velocity distributions are much more disturbed due to the strong flow reversal effects. On the other hand, the reversal in the branch could promote phase separation which could result in an unrealistic high value of S_{c_3}. On the other hand, secondary flow effects may reduce this separation effect. Downstream of the vena contracta secondary flow effects are much more pronounced than in the run and a longer pipe length is required until the flow becomes well developed.

Numerous calculations were made with various assumptions for S_1, S_{c_3}, and S_3 (Reimann & Seeger 1983). The best agreement with data from air–water flow and a horizontal branch was obtained with the assumption of homogeneous flow, that is $S_1 = S_{c_3} = S_3 = 1$, and by using the following expression for C_3:

$$C_3 = \left(1 + \frac{V_1}{V_3} \sqrt{K_{13}} \right)^{-1}. \quad [32]$$

For this case the present model reduces to a homogeneous model (termed PHM) given by

$$\Delta p_{1-3} = \frac{\rho_{h_3}}{\rho_{h_1}} K_{13} \frac{G_1^2}{2\rho_{h_1}} + \frac{\rho_{h_3}}{2} \left[\left(\frac{G_3}{\rho_{h_3}} \right)^2 - \left(\frac{G_1}{\rho_{h_1}} \right)^2 \right]. \quad [33]$$

The main difference between the HM and the PHM is the factor ρ_{h_3}/ρ_{h_1}. The two models become equal for $G_3/G_1 = 1$.

5. TEST SECTION AND MEASUREMENTS

The test loop and the parameter range investigated were described in detail in Part I (see also Seeger 1985). The test section consisted of the horizontal inlet (length $L = 1.85$ m), the run ($L = 3.09$ m), and the horizontal or vertical upward or downward branch (corresponding length 3.2, 2.1, or 0.76 m). All pipes had an inside diameter of 50 mm.

Figure 2 shows for the horizontal branch the locations of the 19 pressure taps (2.5 mm diameter) to measure the pressure gradient along the pipe axis. These taps were located at the pipe bottom to avoid air entrapment, all p lines were purged periodically. The pressure differences could be measured with four parallel differential pressure transducers with different measurement ranges. The outlet signals were time averaged in such a way that statistically stationary results were obtained. In figure 2 typical pressure gradients for two different mass flux ratios G_3/G_1 are shown. Far upstream and downstream of the

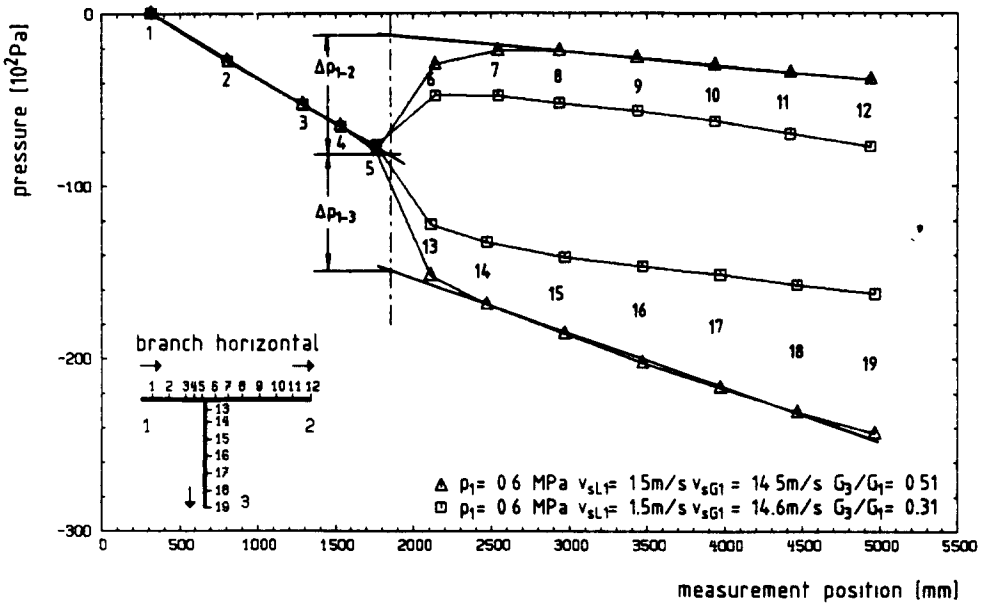

Figure 2. Measured axial pressure in a piping system with a horizontal T-junction.

T-junction there is a constant pressure gradient due to wall friction. The pressure differences at the junction were obtained by extrapolating these gradients to the junction center. For vertical branch directions the frictional pressure drop was determined from the measured value taking into account the gravitational pressure difference.

6. RESULTS

6.1 Single-phase flow

Figure 3 shows the pressure loss coefficients K_{12} and K_{13} for single-phase water flow. The data are generally in good agreement with results obtained by other authors (Gardel

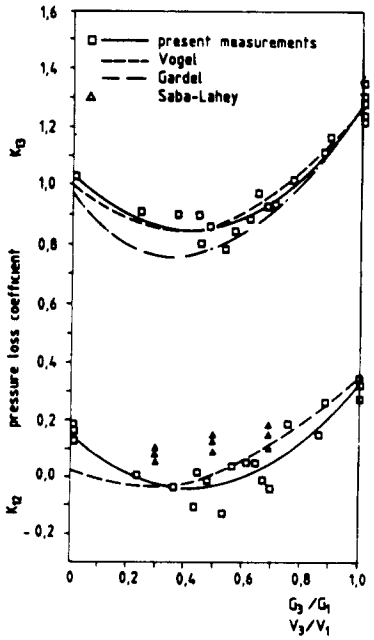

Figure 3. Comparison of pressure loss coefficients K_{12} and K_{13} measured in single-phase flow.

1957; Vogel 1928; Saba & Lahey 1982). The following relationships are used for the further calculations:

$$K_{12} = 0.1571 - 0.9197 \frac{G_3}{G_1} + 1.0901 \left(\frac{G_3}{G_1}\right) \quad [34]$$

for $0 \leq K_{12} \leq 0.24$ and $0.606 \leq K_{12} \leq 1$. In the intermediate range K according to [34] becomes slightly less than 0 which would result in a negative root in [28]. Therefore, in this range K was set to $K = 1$.

$$K_{13} = 1.0369 - 0.9546 \frac{G_3}{G_1} + 1.2123 \left(\frac{G_3}{G_1}\right)^2 . \quad [35]$$

Of course, these relationships do not change if G_3/G_1 is replaced by the ratio of the volumetric flow rates V_3/V_1.

As mentioned in section 3.2, Saba & Lahey used for Δp_{1-2} a relationship different from [1] which reduces for single-phase flow to

$$\Delta p_{1-2} = \frac{K_{12}^*}{2\rho} (G_2^2 - G_1^2) . \quad [36]$$

K_{12}^* is determined from K_{12} by equating [1] and [36]. The solid curve in figure 4 represents the present experiments: K_{12}^* approaches $-\infty$ for $G_3/G_1 = 0$. The figure also contains the experimental results obtained by Saba & Lahey. In their model, which is only valid for $G_3/G_1 \geq 0.3$, Saba & Lahey (1984) recommend a relationship independent of G_3/G_1.

6.2 Two-phase flow

6.2.1 Pressure difference Δp_{1-2}. In figures 5–8 the experimental results are compared with predictions of the following models:

—the present model (PM) according to [27]–[31],

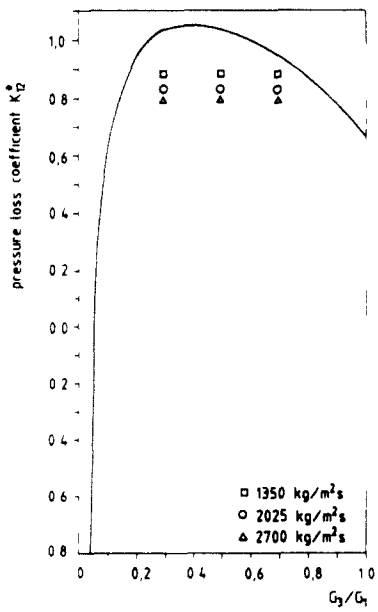

Figure 4 Loss coefficients K_{12}^*.

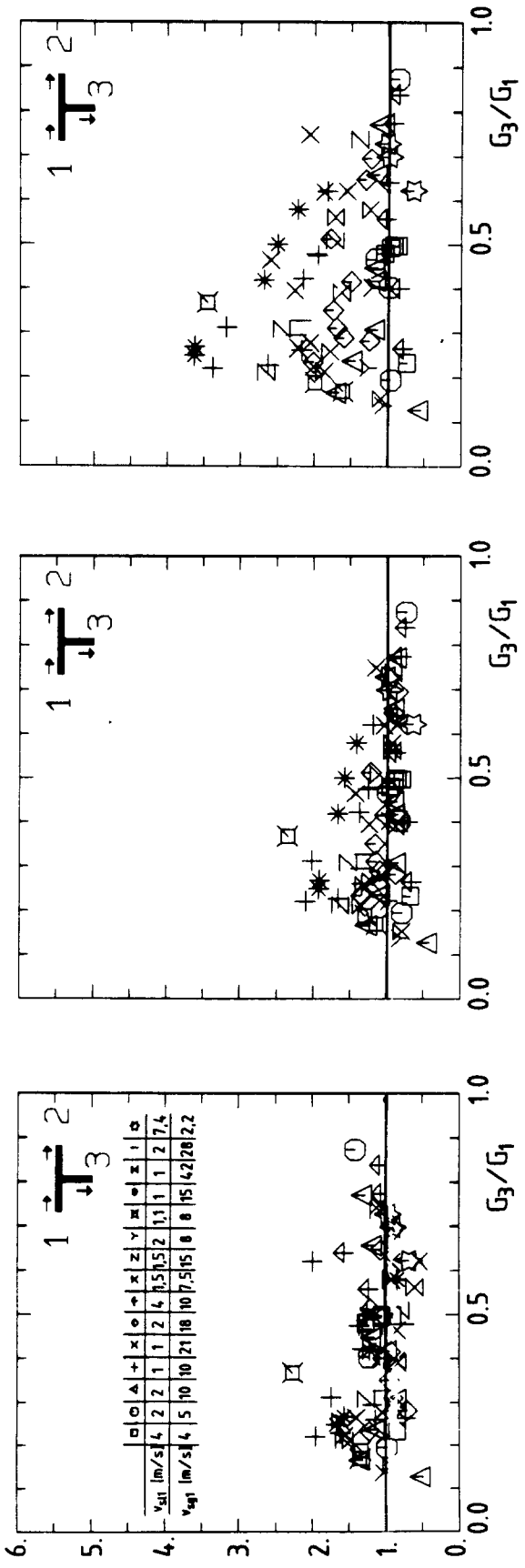

Figure 5 Ratio of predicted to measured run pressure drop for horizontal branch and air–water flow ($p_1 \approx 0.7$ MPa).

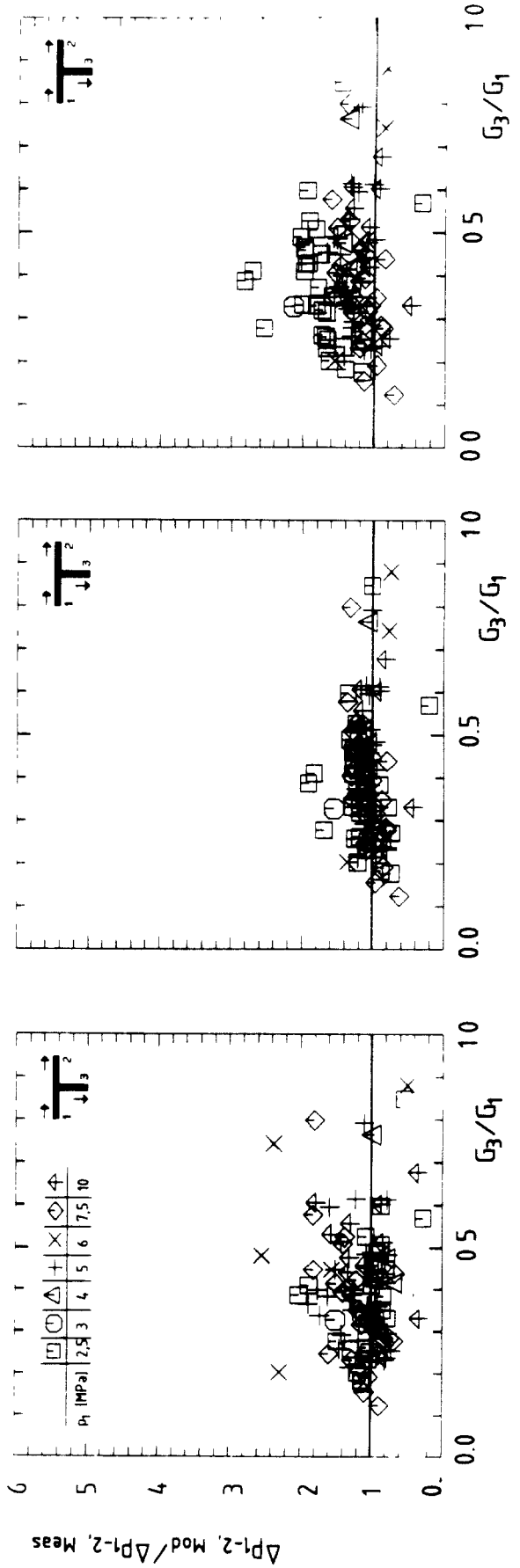

Figure 6 Ratio of predicted to measured run pressure drop for horizontal branch and steam–water flow ($2.5 < p_1 < 10$ MPa)

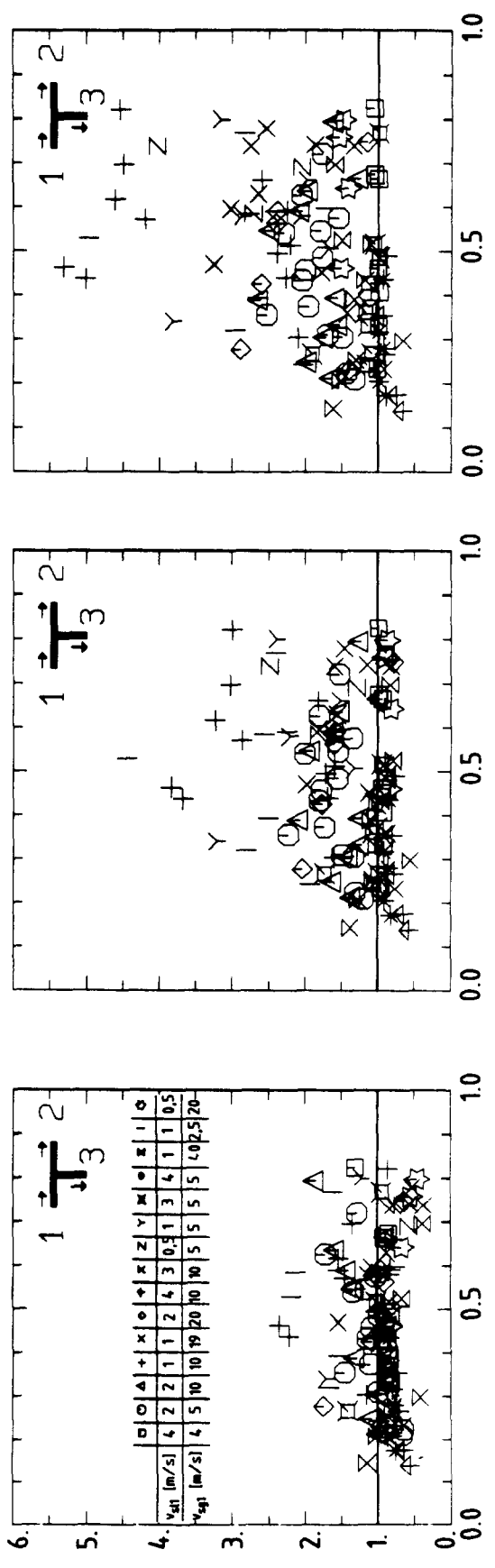

Figure 7 Ratio of predicted to measured run pressure drop for downward branch and air–water flow ($p_1 \approx 0.7$ MPa).

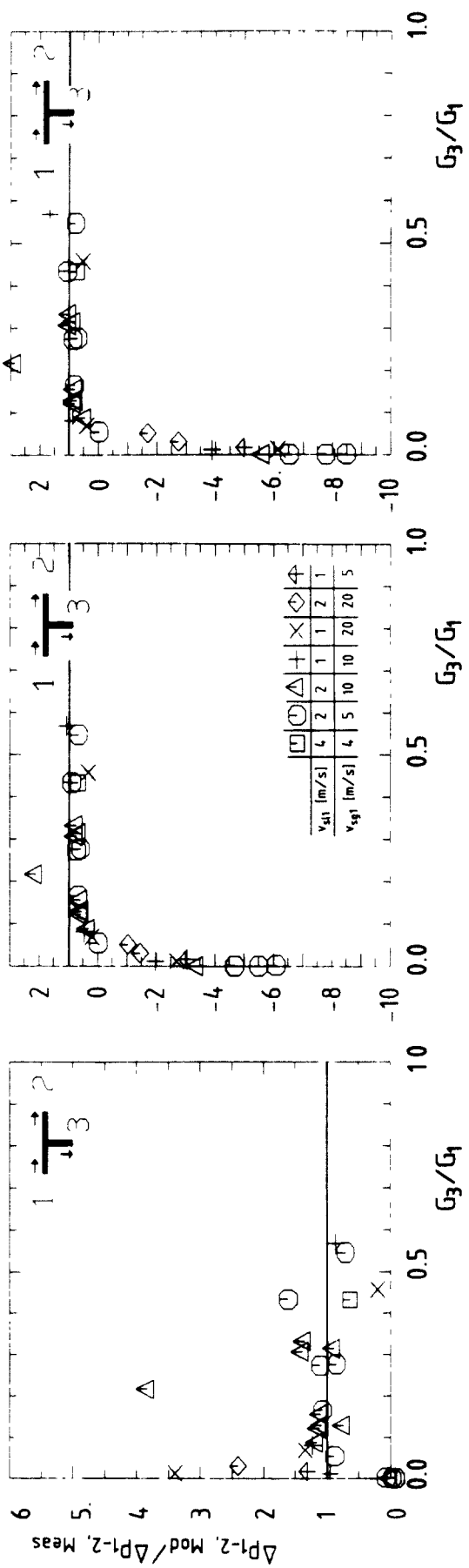

Figure 8 Ratio of predicted to measured run pressure drop for upward branch and air–water flow ($p_1 \approx 0.7$ MPa)

—the model according to [16], listed but not used in the report of Saba & Lahey (1982) and termed Saba–Lahey Slip Model (SLSM). In the present article the momentum density is determined using [22] and [29]–[31],
—the homogeneous model according [18] recommended by Saba & Lahey (termed SLHM).

For all cases, the ratio of the predicted pressure drop $\Delta p_{1-2,\mathrm{Mod}}$ to the measured pressure drop $\Delta p_{1-2,\mathrm{Meas}}$ is presented as a function of the mass flux ratio G_3/G_1. Parameters are the inlet superficial velocities v_{sG_1} and v_{sL_1}.

For horizontal branch and air–water flow (figure 5) the SLHM gives values which are generally too high and scatter most. The two other models agree better with the measurements.

For steam–water flow (figure 6) the SLHM predicts slightly high values; the PM gives a better mean value but the scatter is still great. The SLSM produces the lowest scattering and a good mean value.

For air–water flow and the downward orientated branch (figure 7), the PM has the highest accuracy.

The air–water experiments with the upward branch are predicted by all models with about the same accuracy for $G_3/G > 0.15$. With this branch orientation some of the experiments were performed at very low values of G_3/G_1 (figure 8). Here the PM is superior to the other models.

Figure 9 shows for comparison corresponding graphs based on the experimental data of Saba & Lahey (1982). The PM gives in general high values with a relatively large scatter. The SLSM produces a small scatter but the values are generally too low. The SLHM fits best their data.

6.2.2 Pressure drop Δp_{1-3}. The following models are compared with experimental data:
—the present homogeneous model (PHM) according to [33],
—the homogeneous model (HM) recommended by Saba & Lahey (1982) according to [12],
—the model proposed by Chisholm (1967) (CM) using [11] and [13]–[15].

The irreversible pressure drop $(\Delta p_{1-3})_{\mathrm{irr}}$ is considerably larger than the irreversible pressure drop $(\Delta p_{1-2})_{\mathrm{irr}}$. This is also evident from the pressure loss coefficients in single-phase flow; see figure 3. Therefore, $(\Delta p_{1-3})_{\mathrm{irr}}$ is of large importance and it is favorable to discuss first the experiments where the total pressure drop Δp_{1-3} is equal to $(\Delta p_{1-3})_{\mathrm{irr}}$. This is the case for $G_3/G_1 = 1$, where—as mentioned before—the PHM becomes equal to the HM. Figure 10 shows the air–water results for the horizontal branch as a function of the inlet mass flux G_1 and quality x_1. No model predicts satisfactorily the data. However, the data scatter quite uniformly around a value K given in the figures, approximately independently of G_1 and x_1. It is interesting to note that using the steam–water data of Fitzsimmons (1964), the HM also predicts low values (about 30%). However, the CM, fitting these data predicts values which are about 17% too high compared with the present measurements.

This correction factor K was used by Reimann & Seeger (1983) to modify the expression for $(\Delta p_{1-3})_{\mathrm{irr}}$ in the following way:

$$\Delta p_{1-3} = K^{-1}\,(\Delta p_{1-3})_{\mathrm{irr}} + (\Delta p_{1-3})_{\mathrm{irr}}\,, \qquad [37]$$

with $K = 0.744$ for the HM and PHM and $K = 1.174$ for the CM.

Figure 11 shows the corresponding results for steam–water flow at G_3/G_1, using [37]. The data scatter around the correct value. The dependency of the result on the system pressure is not clear due to the small number of experiments at each pressure level. Therefore, a more sophisticated dependence on the system pressure was not derived.

For the downward branch and air–water flow, only four test points with $G_3/G_1 = 1$ were performed. Again, the agreement is reasonably good if [37] is used (figure 12).

Figure 13 shows the results for the upward branch flow: with decreasing mass flux G_1 or increasing quality x, the derivations increase. For this flow orientation the phase sepa-

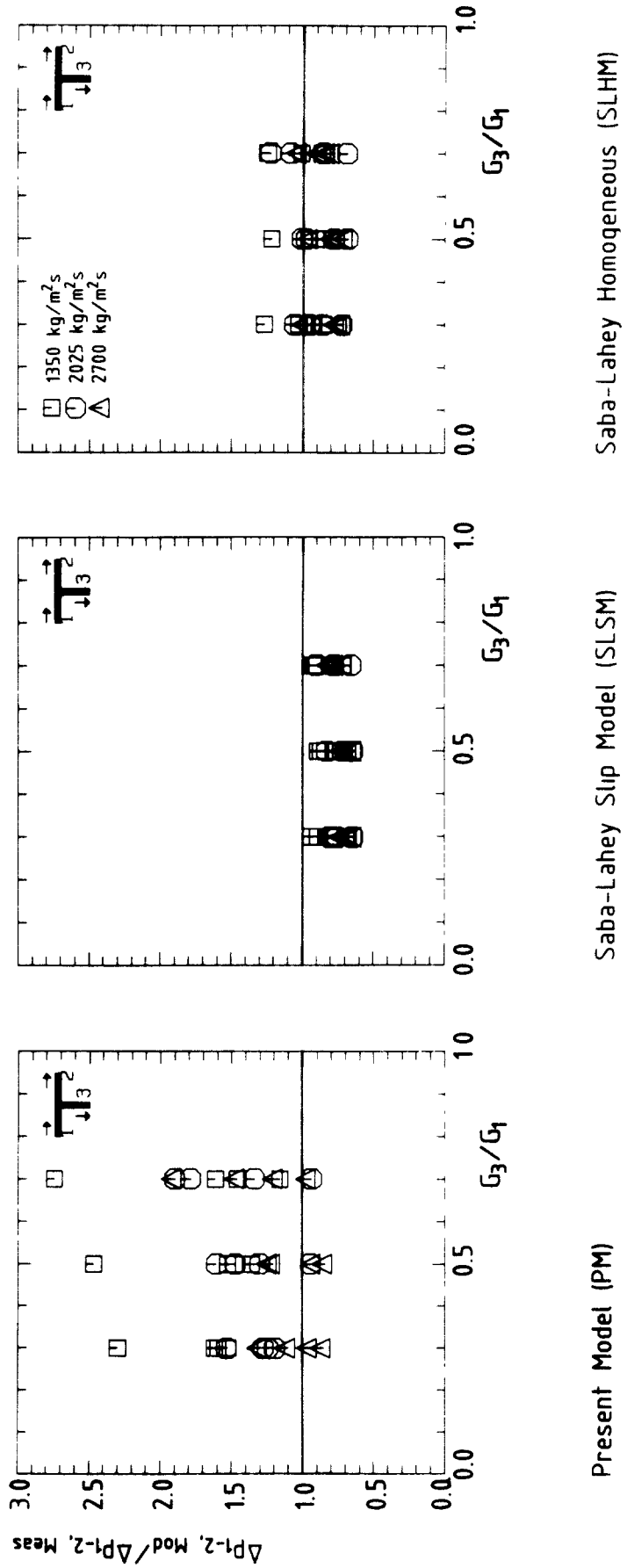

Figure 9 Ratio of predicted to measured run pressure drop for horizontal branch and air - water flow ($p_1 \simeq 0.15$ MPa); experimental data from Saba & Lahey

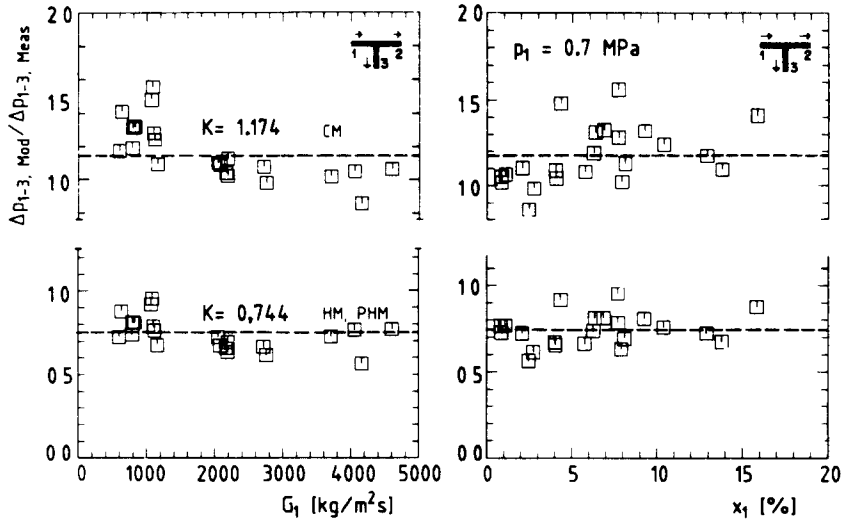

Figure 10. Ratio of predicted to measured branch pressure drop for $G_3/G_1 = 1$, horizontal branch and air–water flow.

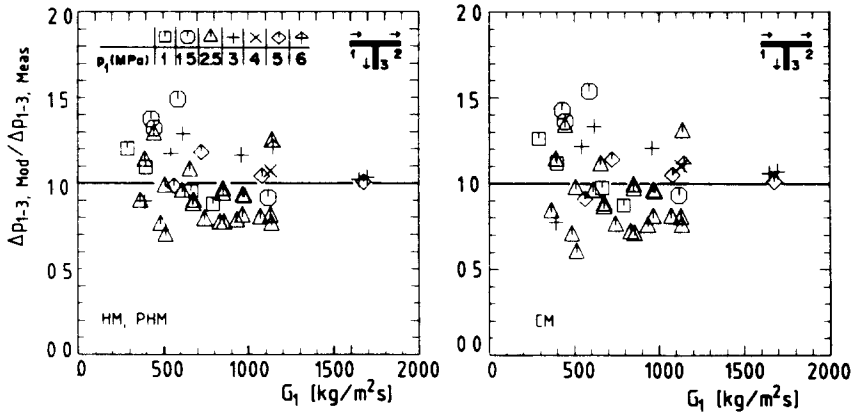

Figure 11 Ratio of predicted to measured branch pressure drop for $G_3/G_1 = 1$, horizontal branch and steam–water flow.

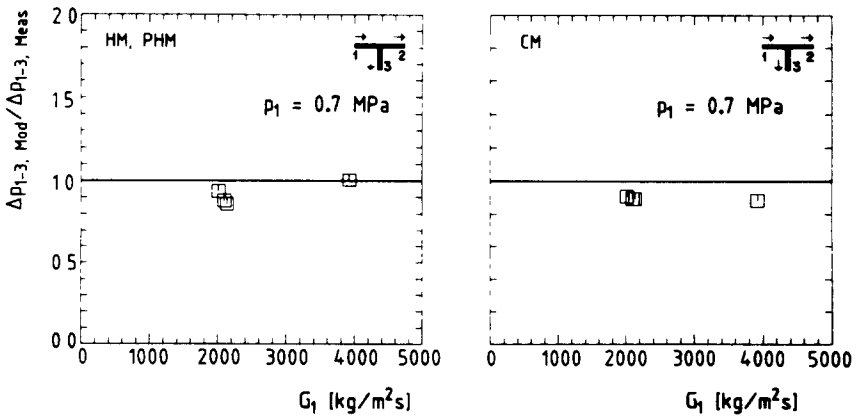

Figure 12 Ratio of predicted to measured branch pressure drop for $G_3/G_1 = 1$, downward branch and air–water flow.

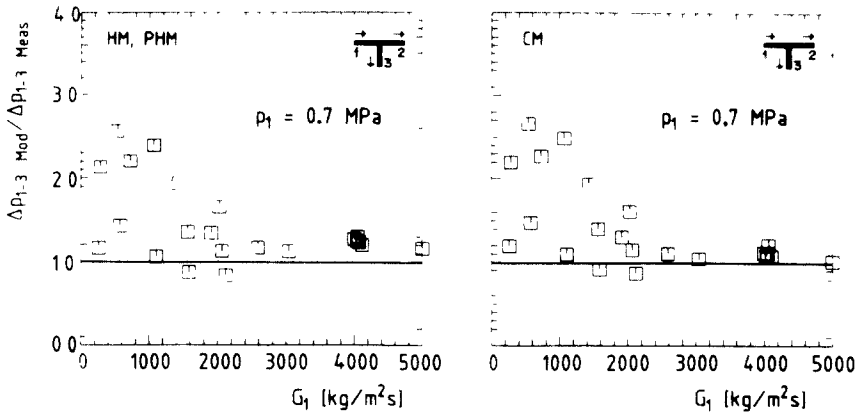

Figure 13 Ratio of predicted to measured branch pressure drop for $G_3/G_1 = 1$, upward branch and air–water flow

ration effects in the branch become very important even for large distances downstream of the branch inlet [compare Part I and Seeger *et al.* (1985)]. Therefore, the assumption of homogeneous flow is in general not justified.

Figures 14–17 show the results for split ratios $0 < G_3/G_1 < 1$. Figure 14 contains air–water data with the horizontal branch presented previously (Reimann & Seeger 1983). The results of the HM and CM are very similar: the models predict well the experimental results in the range $0.6 < G_3/G_1 < 1$, but overpredict the experiments at lower values of G_3/G_1. This tendency does not change significantly if the dependence $K_{13} = f(V_3/V_1)$ is used instead of $K_{13} = f(G_3/G_1)$. The PHM predicts the measurements much better in the lower range of the mass flux ratio.

Figure 15 shows the comparison with the steam–water experiments. Again the HM and CM models deviate strongly for $G_3/G_1 < 0.6$. The PHM starts to deviate at considerably lower mass flux ratios ($G_3/G_1 < 0.3$). A systematic dependence on system parameters can not be seen clearly.

Figure 16 contains air–water data for the downward branch. The PHM is superior in the total range of G_3/G_1.

For the upward branch (figure 17) all models fail; the CM (not shown) gives values similar to the HM. The deviations given by the PHM model are smallest (note the different scales of the ordinate). The deviations are again caused mainly by the separation effects in the branch which increase with decreasing branch mass flux G_3

If the assumption of homogeneous flow in the branch is abandoned, i.e. [23] and [24] are used, and S_3 is determined with [28]–[31] the results shown on the right-hand side of figure 17 are slightly improved.

Figure 18 compares the results of the models with the experimental data from Saba & Lahey (1982). These authors did not perform two-phase flow measurements at $G_3/G_1 = 1$. Therefore, the correction factor K from the present experiments was used. The PHM model gives the best mean value and the lowest data scatter. If a correction factor $K = 1$ is taken, as done by Saba & Lahey, the results are shifted somewhat, but the agreement is not improved remarkably

7 SUMMARY

The model presented in this article predicts better in general the experimental results compared to previous models for all branch orientations and fluid systems. The results for vertical upward flow, however, are not satisfactory because of the complex flow configuration due to phase separation. Further investigations including for example, global or local void fraction measurements, are required for this case.

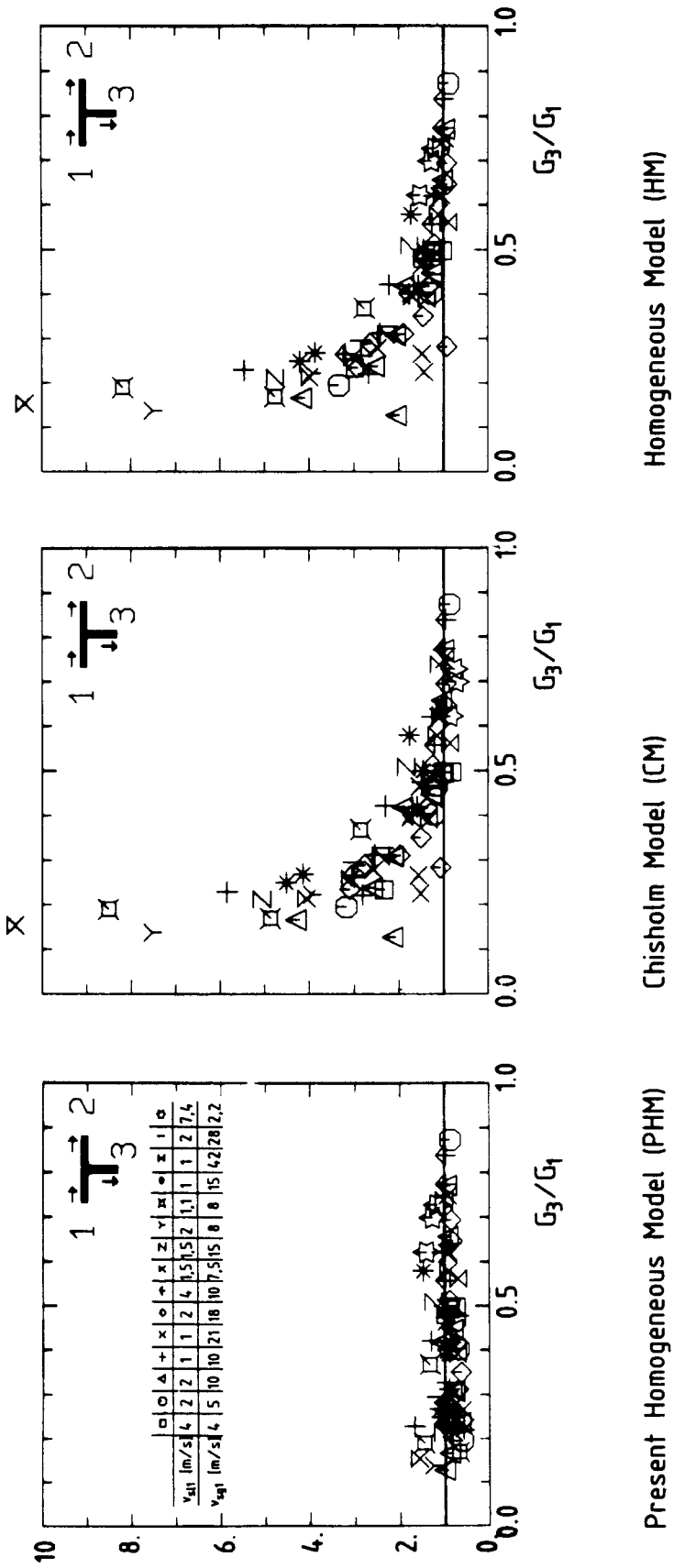

Figure 14 Ratio of predicted to measured branch pressure drop for horizontal branch and air–water flow

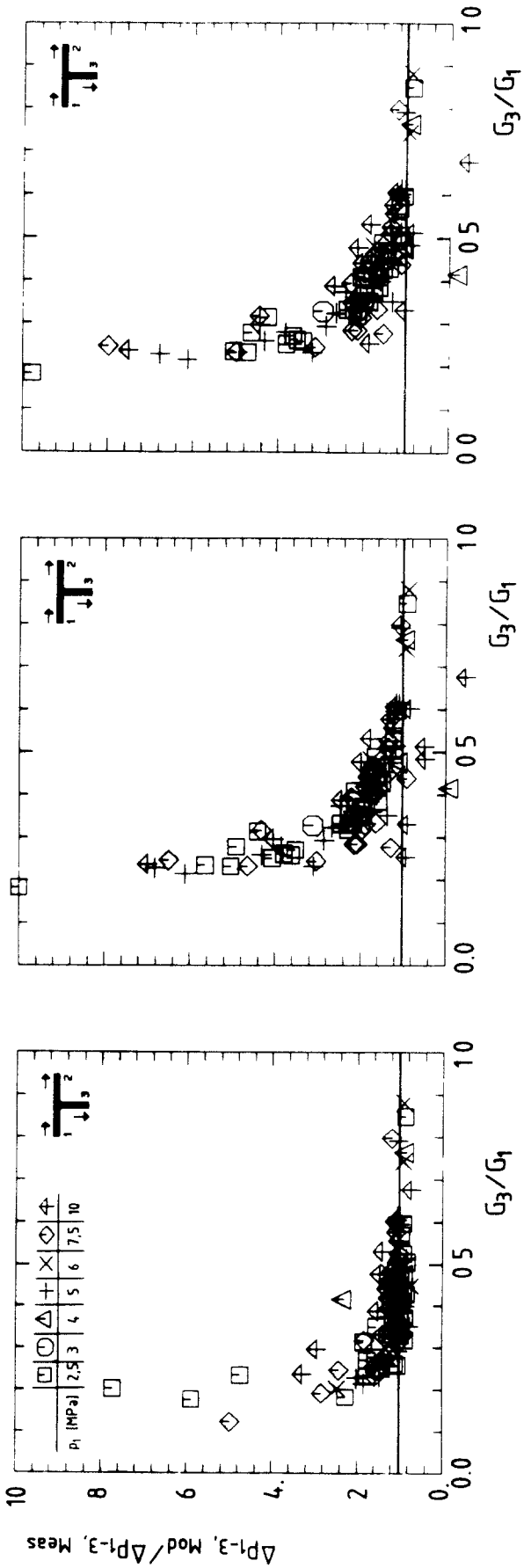

Figure 15. Ratio of predicted to measured branch pressure drop for horizontal branch and steam–water flow

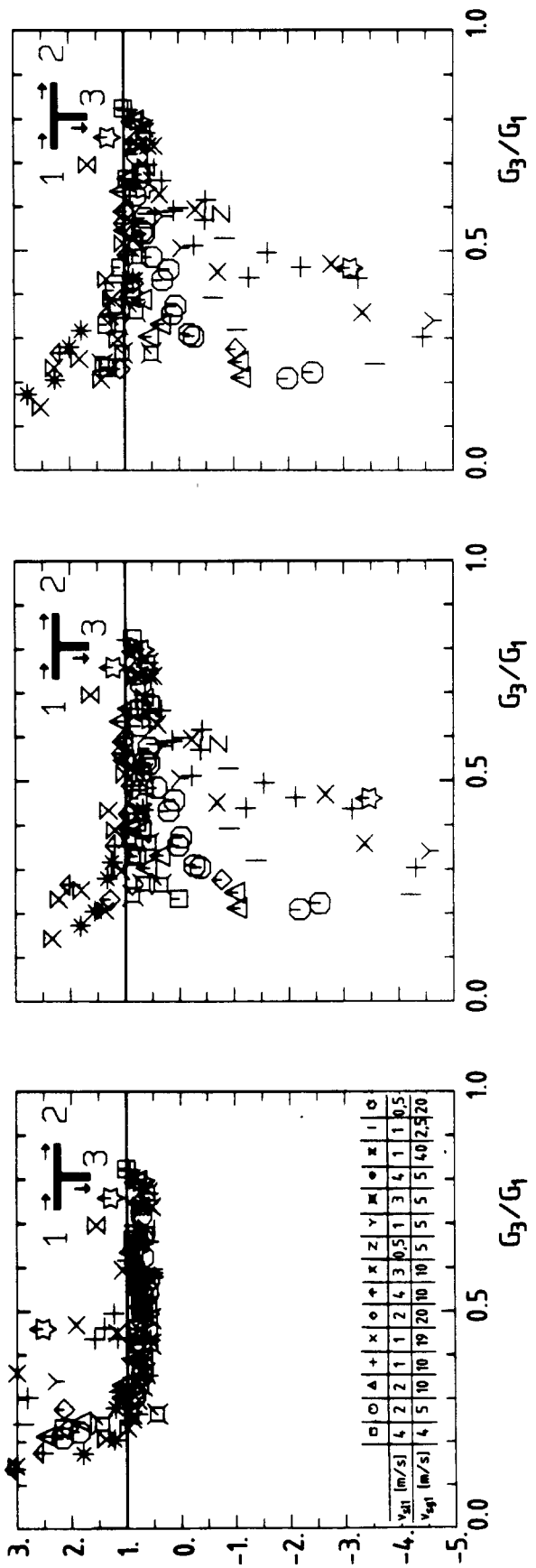

Figure 16. Ratio of predicted to measured branch pressure drop for downward branch and air–water flow.

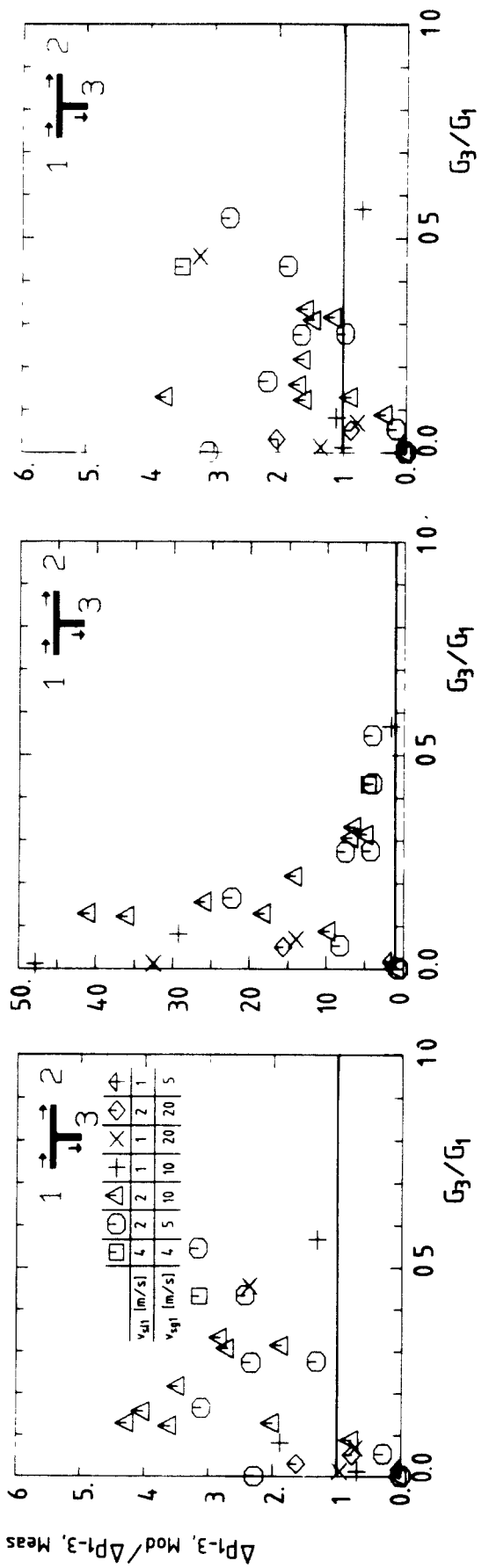

Figure 17 Ratio of predicted to measured branch pressure drop for upward branch and air - water flow

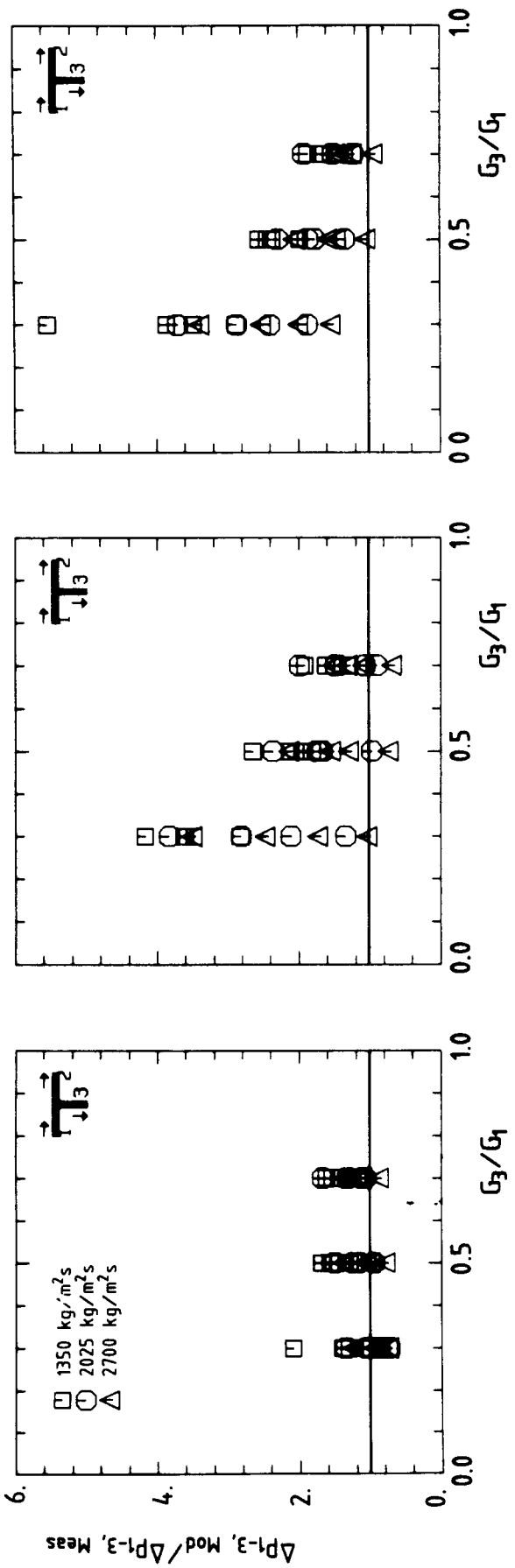

Figure 18. Ratio of predicted to measured branch pressure drop for horizontal branch and air–water flow. Experiments from Saba & Lahey.

REFERENCES

CHISHOLM, D. 1967 Pressure losses in bends and tees during steam–water flow. NEL Report 318, National Engineering Lab., Glasgow, Scotland.

COLLIER, J. G. 1976 Single-phase and two-phase flow behavior in primary circuit components. *Proc. NATO Advanced Institute on Two-phase Flow and Heat Transfer*, Vol. 1, pp. 313–365, Hemisphere Corp.

FITZSIMMONS, D. E. 1964 Two-phase pressure drop in piping components. HW 80970 REV1, General Electric Hanford Laboratories, Richland, Washington.

GARDEL, A. 1957 Les pertes de charges dans les écoulements au travers de branchements en té. *Bull. Tech. Suisse Romande* **9**, 122–130; **10**, 143–148.

HACKESCHMIDT, M. 1970 *Grundlagen der Strömungstechnik*. VEB Deutscher Verlag, Leipzig, DDR.

KATSAOUNIS, A., AUST, E., FUERST, H. D. & SCHULTHEISS, G. F. 1983 Pressure drop in T-junctions with liquid and gas–liquid flow. In: *Heat Exchangers for Two-Phase Applications*. Presented at the *21st National Heat Transfer Conference*, Seattle, Washington, July 24–28.

REIMANN, J. & SEEGER, W. 1983 Two-phase pressure drop in a dividing T-junction. *The Mechanics of Gas Liquid Flow Systems, Euromech Colloquium 176*, Villard de Lans, France, Sept. 21–23.

ROUHANI, Z. 1969 Modified correlations for void and two-phase pressure drop. AE-RTV-841.

SABA, N. & LAHEY, R. T. 1982 Phase separation phenomena in branching conduits. NUREG/CR-2590, Department of Nuclear Engineering, Rensselaer Polytechnic Institute, Troy, NY.

SABA, N. & LAHEY, R., Jr. 1984 The analysis of phase separation phenomena in branching conduits. *Int. J. Multiphase Flow* **10**, 1–20.

SALLET, D. W. & POPP, M. 1983 Experimental investigation of one- and two-phase flow through a tee-junction; physical modelling of multiphase flow. Coventry, England, 19–21 April.

SEEGER, W. 1985 Untersuchungen zum Druckabfall und zur Massenstromverteilung von Zweiphasenströmungen in rechtwinkligen Rohrverzweigungen. Dissertation, Universität Karlsruhe, KfK 3876.

SEEGER, W., REIMANN, J. & MÜLLER, U. 1985 Phase separation in a T-junction with a horizontal inlet. *2nd Int. Conf. on Multi-Phase Flow*, London, England, 19–21 June.

VDI-Wärmeatlas (Hrsgg.), 1984 *Verein Deutcher Ingenieure, VDI-Gesellschaft für Verfahrenstechnik und Chemieingenieurwesen (GVC)*. VDI-Verlag, Düsseldorf.

VOGEL, G. 1928 *Untersuchungen über den Verlust in rechtwinkligen Rohrverzweigungen*, Heft 2, pp. 61–64. Mitteilung des hydr. Inst. der T.H. München.